

AD-A068 876

PURDUE UNIV LAFAYETTE IND
COMPUTERIZED DETECTION AND CLASSIFICATION USING ARTIFICIAL INTE--ETC(U)
AUG 70 E A PATRICK, L SHEN, R AGNEW

F/G 17/1

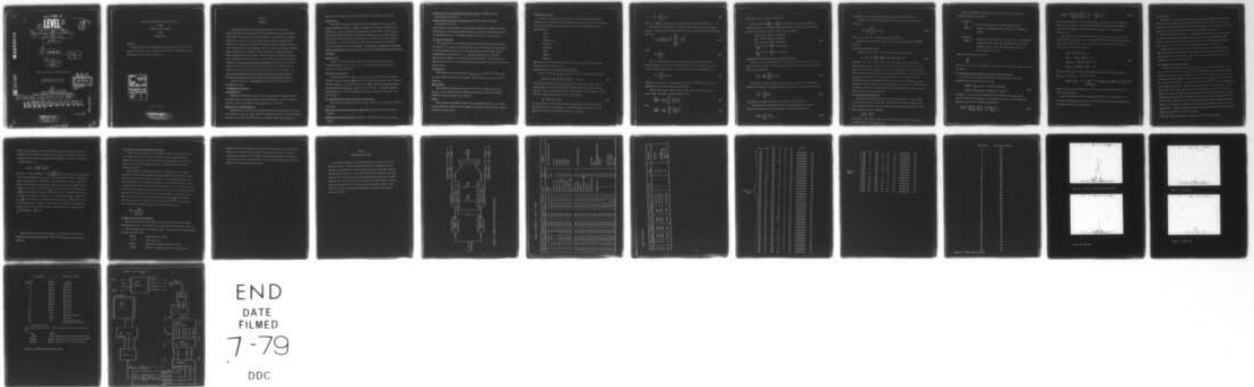
N00024-70-C-1248

NL

UNCLASSIFIED

| OF |

AD
A068876



END
DATE
FILMED
7-79
DDC

GOOD
MOST Project -4

Unclassified

LEVEL II

1 p.5.

9
INTERIM ENGINEERING REPORT

6
COMPUTERIZED DETECTION AND CLASSIFICATION
USING
ARTIFICIAL INTELLIGENCE
AND
ESTIMATION

11
10 August 1970

12 28p.

10
E.A. Patrick
L./Shen
R./Agnew

Purdue University, Lafayette, Indiana

DEPARTMENT OF THE NAVY
Naval Ship Systems Command

DDC
RECEIVED
MAY 23 1979
REGISTRY
D

15
Contract N00024-70-C-1248

Project Serial No. SF 11-121-106, Task 08637

16 F11121 17 SF11121 106

This document is subject to special export controls and each transmittal to foreign governments or foreign nationals may be made only with prior approval of Commander, Naval Ship Systems Command, Code 001C3.

Copy No. 1

DISTRIBUTION STATEMENT A

Approved for public release;
Distribution Unlimited

291650

AD A 068876

DDC FILE COPY

DDC

88-15

JP

COMPUTERIZED DETECTION AND CLASSIFICATION
USING
ARTIFICIAL INTELLIGENCE
AND
ESTIMATION

ABSTRACT:

sonar
→ Automatic Detection and Classification cannot be had by estimation alone but it can be had by estimation plus artificial intelligence where the latter reflects problem knowledge. ←

AUTHORITY BY	
DTIC	DTIC SOURCE <input checked="" type="checkbox"/>
DDI	DDI SOURCE <input type="checkbox"/>
MANUSCRIPT	<input type="checkbox"/>
IDENTIFICATION	
<i>Per H.S. on file</i>	
BY	
DISTRIBUTION/AVAILABILITY CODES	
Dist.	AVAIL. CODE/W. SPECIAL
A	

[first]

DISTRIBUTION STATEMENT A
Approved for public release;
Distribution Unlimited

Part I

FORWARD

A carefully developed body of knowledge concerning estimation in sonar detection and classification has been developed and made available to Naval Ships Systems Command in previous reports. In section I we summarize definitions of measurement space, feature space, decision space, and the decision rule, and we comment on the generalized k nearest neighbor decision rule, nonparametric feature selection, cluster mapping, and the Bayes solution. Then, in Chapter II, we introduce the new approach to pattern recognition which provides for inserting problem knowledge into the decision making process. This approach, although not so new in "idea" is very new in "action". We discuss nonlinear mappings we have discovered which can be used to insert a priori problem knowledge. We show how features can be designed first for submarine targets and then for specific kinds of nonsubmarine targets. By using a priori problem knowledge, pattern recognition can take place with no training samples; the training samples then add ice cream to the pie.

Section IV provides an introduction to performance results after processing Rogers data.

I Theoretical Foundation

A. Introduction

Appropriate definitions, notation, and operations have been fairly well established for computerized detection and classification. In this section we provide a tutorial and indicate where improvements can be made.

Measurement or Observation Space

Measurements of a sonar echo or sequence of sonar echoes provide components of a vector $\underline{x} = [x_1, x_2, \dots, x_L]$ called the observation vector. These measurements are made on the audio waveform, video scan waveform, along with associated

measurements of target range R , true bearing θ , and target track aspect ψ .

Feature Space

The process of obtaining features from the observation vector \underline{x} involves inserting problem knowledge. Features important for detecting a submarine are different from features important for detecting a nonsubmarine. For example, a nonsubmarine target may consist of multiple targets in range, bearing scan, or both; features which measure these properties are thus important for detecting nonsubmarines. On the other hand, an estimate target length is an important feature for detecting submarine targets. It is important to provide that features useful in detecting one type of target are not a nuisance in detecting another type of target.

Decision Space

Simply, the decision space consists of M classes with corresponding a priori probabilities P_i , $i = 1, 2, \dots, M$. We may consider the decision space one dimensional with M points.

The Unique Decision Rule

Loosely speaking, the unique decision rule is a Bayes, minimum conditional risk rule where the density $f(\underline{x}|i)$ and a priori class probability P_i are calculated for all M classes. It is necessary to learn $f(\underline{x}|i)$ using both problem knowledge and training vectors $\underline{x}_1^i, \underline{x}_2^i, \dots, \underline{x}_{n_i}^i$ for this i^{th} class. The density $f(\underline{x}|i)$ is characterized by a set of parameters \underline{b}_i where \underline{b}_i is related to the features for the i^{th} class.

B. The New Pragmatic Approach to Pattern Recognition

We at Purdue University have made several contributions to pattern recognition including:

The Generalized K-Nearest Neighbor Decision Rule, published in Information and Control

Non-Parametric Feature Selection, published in IEEE Transactions on Information Theory

Cluster Mapping with Experimental Computer Graphics, published in IEEE transactions on Computers.

Bayes Solutions to Pattern Recognition, published in IEEE transactions on Information Theory.

Now, however, we are working on a more advanced approach to pattern recognition which provides for inserting problem knowledge along with training samples into the automation process. Subsequent sections will describe the procedure.

II The New Procedure

The approach is to use problem knowledge to transform observation vectors x^i from class i to a lower dimensional space where the features are uncorrelated. A nonlinear transformation must be constructed for each class; this nonlinear transformation may be thought of as resulting ultimately in a nonlinear matched filter which can be updated using training samples. The procedure is best described in terms of the following operations used to construct the nonlinear transformations.

Within Subset

This operation selects measurements $x_{s_1}, x_{s_2}, \dots, x_{s_L}$ from the s^{th} sonar ping to which nonlinear operations are applied. These measurements are in the s^{th} vector x_s .

Between Subset

This operation selects measurements from each of a sequence of v pings x_1, x_2, \dots, x_v to which nonlinear operations are applied. One such nonlinear operation is the "Starlight" type operation.

Region

This operation selections a region of the observation space V_L . Any points in this region are processed with a sequence of operations specialized to samples restricted to this region.

Correlation Inserter

A linear or nonlinear function of measurements selected by operations "within subset" or "between subset" gives rise to a new feature. The following is a list of nonlinear functions which may or may not be directly used in sonar problems:

- ratio
- sum
- weighted sum
- blanking
- quadratic
- ring
- product
- subgroup

More specialized nonlinear relationships have been found from sonar problem knowledge and are described next.

A. Designing Nonlinear Filters for Detecting Subs

Measurement vectors x_1, x_2, \dots, x_v are taken for v successive pings with

$$x_r = [\hat{l}_r, \hat{E}_r, \hat{NP}_r, \hat{\psi}_r, \hat{R}_r, \hat{\theta}_r, \hat{N}_r], \quad r = 1, 2, \dots, v \quad (1)$$

where \hat{l}_r is an estimate of target length, \hat{E}_r of target echo energy, \hat{NP}_r of noise energy, $\hat{\psi}_r$ of aspect angle, \hat{R}_r of target range, $\hat{\theta}_r$ of target bearing, and \hat{N}_r of number of target highlights. When the same class of target is active for all v echos, the sequence vector of measurements

$$\hat{x}_v = [x_1, x_2, \dots, x_v] \quad (2)$$

is constructed. If there are L entries in x_r then there are Lv entries in \hat{x}_v and they can't be uncorrelated. We know that target length l is a fixed parameter and it is reasonable to use the sum operation,

$$\hat{l} = \frac{1}{v} \sum_{r=1}^v \alpha_r \hat{l}_r \quad (3)$$

where $\alpha_r = \hat{E}_r / \hat{NP}_r$ is an estimate of signal/noise ratio for the r^{th} echo.

The target reflectivity is a reasonable feature characterizing submarine targets. An estimator for target reflectivity σ is signal/noise ratio normalized for range,

$$\hat{\sigma} = \left(\frac{\hat{\text{signal}}}{\hat{\text{noise}}} \right) (\hat{R})^2 = \frac{\sum_{r=1}^v \hat{E}_r}{v \sum_{r=1}^v \hat{NP}_r} (\hat{R})^2 \quad (4)$$

where

$$\hat{R} = \frac{1}{v} \sum_{r=1}^v \hat{R}_r \quad (5)$$

The number of highlights is another reasonable feature characterizing submarine targets. Since the number of highlights in a submarine echo depends on the submarine aspect angle, an estimator for the number of highlights is

$$\hat{N} = \frac{1}{v} \sum_{r=1}^v \hat{N}_r \cos \hat{\psi}_r \quad (6)$$

where \hat{N}_r is a measurement of the number of peaks in the r^{th} echo and $\hat{\psi}_r$ is an estimate of target aspect angle on the r^{th} echo.

Because sub-targets can have certain range rates and rate of change of aspect angle, two other reasonable features are

$$\left(\frac{\Delta R}{\Delta t} \right) = \frac{1}{(v-1)} \sum_{r=1}^{v-1} \frac{R_{r+1} - R_r}{t_{r+1} - t_r} \quad (7)$$

and

$$\left(\frac{\Delta \psi}{\Delta t} \right) = \frac{1}{(v-1)} \sum_{r=1}^{v-1} \frac{\hat{\psi}_{r+1} - \hat{\psi}_r}{t_{r+1} - t_r} \quad (8)$$

where $t_{r+1} - t_r$ is the time between pings.

Features \hat{l} , $\hat{\sigma}$, \hat{N} , $\left(\frac{\Delta R}{\Delta t}\right)$, and $\left(\frac{\Delta \psi}{\Delta t}\right)$ are significant features for detecting submarine targets. To achieve a spherical density, we will need the following estimates of variances of these features for sub targets:

$$\begin{aligned} \hat{s}_l &= \text{variance } (\hat{l}) \text{ for sub-targets} \\ \hat{s}_\sigma &= \text{variance } (\hat{\sigma}) \text{ for sub-targets} \\ \hat{s}_N &= \text{variance } (\hat{N}) \text{ for sub-targets} \\ \hat{s}_{\left(\frac{\Delta R}{\Delta t}\right)} &= \text{variance } \left(\frac{\Delta R}{\Delta t}\right) \text{ for sub-targets} \\ \hat{s}_{\left(\frac{\Delta \psi}{\Delta t}\right)} &= \text{variance } \left(\frac{\Delta \psi}{\Delta t}\right) \text{ for sub-targets} \end{aligned} \tag{9}$$

B. Designing Non-linear Filters for Detecting Nonsubs

Because the number of highlights is not any particular fixed value for many types of nonsubs, a reasonable additional feature for nonsubs is the average change in number of highlights,

$$\left(\Delta \hat{N}\right) = \frac{1}{(v-1)} \sum_{r=1}^{v-1} (\hat{N}_{r+1} - \hat{N}_r) \tag{10}$$

Some nonsubs produce multiple targets in range. Therefore a reasonable feature is the number of detected targets in range, TR, an estimate for which is,

$$\left(\hat{TR}\right) = \frac{1}{v} \sum_{r=1}^v \left(\hat{TR}\right)_r \tag{11}$$

with $\left(\hat{TR}\right)_r$ the number of targets in range on the r^{th} echo return.

In like manner, the number of targets in bearing $T\theta$, is a reasonable feature for certain kinds of nonsubs where a reasonable estimate is

$$\left(\hat{T\theta}\right) = \frac{1}{v} \sum_{r=1}^v \left(\hat{T\theta}\right)_r \tag{12}$$

with $(\hat{TR})_r$ the number of targets in bearing on the r^{th} echo return.

For certain nonsubs, the echo length may change such that a reasonable feature is

$$\hat{\Delta e} = \frac{1}{v-1} \sum_{r=1}^{v-1} |\hat{e}_{r+1} - \hat{e}_r| \quad (13)$$

where \hat{e}_r is the estimated echo length for the r^{th} echo.

The features specifically selected for nonsubs thus are $(\hat{\Delta N})$, (\hat{TR}) , $(\hat{T\theta})$, and $(\hat{\Delta e})$.

C. Combined Set of Features

The vector of combined features for subs and nonsubs is thus

$$\underline{y} = [\hat{l}, \hat{\sigma}, \hat{N}, (\frac{\hat{\Delta R}}{\hat{\Delta t}}), (\frac{\hat{\Delta t}}{\hat{\Delta t}}), \vdots (\hat{\Delta N}), (\hat{TR}), (\hat{T\theta}), \hat{\Delta e}] \quad (14)$$

where the ones in the first segment of the partition are the sub-features (denoted \underline{y}_s) and those in the second segment are the nonsub features (denoted \underline{y}_{ns}). This new feature vector \underline{y} has features (in \underline{y}_{ns}) specially designed for detecting non-submarine targets. Because there undoubtedly are correlations between \underline{y}_s and \underline{y}_{ns} , it is not wise to use \underline{y} as the feature vector unless a priori knowledge about these correlations is introduced. Put differently, \underline{y}_{ns} would contribute nuisance features when trying to detect a submarine. In the following section it is shown how a very elementary form of correlation can be inserted by using conditional density functions.

D. Second Level of Correlation

The features in \underline{y} (15) may not have spherical statistics. First of all, \hat{l} and $\hat{\sigma}$ are correlated for nonsubs. We know that for nonsubs, both \hat{l} and $\hat{\sigma}$ can be larger than values for subs or both can be smaller than values for subs. This suggests using the new feature

$$\sqrt{(\hat{l})^2 + (\hat{\sigma})^2}$$

for nonsubs. This feature might also be satisfactory for subs. Too large or too small values would signify a sub.

The features (\hat{TR}) and $(\hat{T\theta})$ can be used to "adapt" the construction of certain new features as follows:

If $(\hat{TR}) > 1$
 or $(\hat{T\theta}) > 1$, then observe the change in $(\hat{\sigma})$ among the several targets. A significant change indicates a nonsubmarine target.

If $(\hat{TR}) > 1$
 $(\hat{T\theta}) > 1$, then observe the pair $(\hat{l}, \hat{\sigma})$ pair for change. Significant difference of this pair from sub-values indicates a non-submarine target. Also, the average value of \hat{l} over these targets can be used.

Another new feature for nonsubs is

$$\frac{\hat{l}}{(\hat{\Delta N})}$$

because, for nonsubs, we expect $(\hat{\Delta N})$ to be increased if the target length estimator \hat{l} increases.

E. Introducing Correlation Using Conditional Density Functions

Let s index the sub-class and ns index the nonsub class. The class conditional densities of \underline{y} can be written,

$$\begin{aligned} p(\underline{y}|s) &= p(\underline{y}_s, \underline{y}_{ns}|s) = p(\underline{y}_s|s, \underline{y}_{ns}) p(\underline{y}_{ns}|s) \\ p(\underline{y}|ns) &= p(\underline{y}_s, \underline{y}_{ns}|ns) = p(\underline{y}_s|\underline{y}_{ns}, ns) p(\underline{y}_{ns}|ns) \end{aligned} \quad (15)$$

Let $d(\underline{y}_s) = i$ mean that the decision rule using feature vector \underline{y}_s decides class i and similarly for $d(\underline{y}_{ns})$. Then the Bayes framework for dimensionality reduction suggests the following approximations:

$$p(\underline{y}|s) \approx \begin{cases} p(\underline{y}_s|s, d(\underline{y}_{ns}) = s), & d(\underline{y}_{ns}) = s \\ p(\underline{y}_s|s, d(\underline{y}_{ns}) = ns), & d(\underline{y}_{ns}) = ns \end{cases} \quad (16a)$$

$$p(\underline{y}|ns) = \begin{cases} p(\underline{y}_{ns}|ns, d(\underline{y}_s) = ns), & d(\underline{y}_{ns}) = ns \\ p(\underline{y}_{ns}|ns, d(\underline{y}_s) = s), & d(\underline{y}_{ns}) = s \end{cases} \quad (16b)$$

We see from (16a) how the non-sub features \underline{y}_{ns} contribute in a simple way to detecting a submarine. Eq.'s (16) suggest the Block diagram shown in Figure 1 where all the nonlinear a priori knowledge has been used to construct the decision rule.

Because nonlinear functions have been used to design \underline{y}_s and \underline{y}_{ns} we suspect that the statistics of the class conditional densities on the right handside (16) are spherical and unimodal. Thus we represent these densities with Gaussian functions. Define the mean vectors,

$$\begin{aligned} \underline{m}_{sss} &= E[\underline{y}_s | s, d(\underline{y}_{ns}) = s] \\ \underline{m}_{ss,ns} &= E[\underline{y}_s | s, d(\underline{y}_{ns}) = ns] \\ \underline{m}_{ns,ns,ns} &= E[\underline{y}_{ns} | ns, d(\underline{y}_s) = ns] \\ \underline{m}_{ns,ns,s} &= E[\underline{y}_{ns} | ns, d(\underline{y}_s) = s] \end{aligned} \quad (17)$$

Likewise, define the corresponding diagonal covariance matrices $\underline{\Sigma}_{sss}$, $\underline{\Sigma}_{ss,ns}$, $\underline{\Sigma}_{ns,ns,ns}$, and $\underline{\Sigma}_{ns,ns,s}$. Then, for example,

$$p(\underline{y}_s | s, d(\underline{y}_{ns}) = s) = \frac{1}{\frac{5}{(2\pi)^2 |\hat{\Sigma}_{sss}|^{\frac{1}{2}}}} \exp\left[-\frac{1}{2}(\underline{y}_s - \underline{m}_{sss}) \underline{\Sigma}_{sss}^{-1} (\underline{y}_s - \underline{m}_{sss})\right] \quad (18)$$

where 5 is the dimensionality of \underline{y}_s and estimated mean vectors and covariance matrices are indicated.

This new approach to pattern recognition is quite viable because we are learning more about sonar every day. We propose to continue its development with the objective of improving performance.

III. Data Base

The data base currently being used is from the Rogers Data Base obtained from ARL, Austin, Texas, 6/21/1970. This data is recorded in Figure 2. The PME Reel inclusion corresponds to the corresponding tape at Purdue. Some of the measurements, speed, class, aspect, and number of pings, are included in this table.

After using this Rogers data, we expect to process Sarsfeld data where ranges are between 2,000 yards and 10,000 yards with some as far as 40,000 yards (subs only). For nonsubs, the maximum range is 7,000 yards. All the Sarsfeld data is 2 m.s., RDT, c.w; tracks are mostly straight line but some are circling.

Another source of data is Witek data involving ranges out of 20,000 yards. This data involves very large sequences for the same target (200-300 pings), for both submarines and nonsubmarines. The Witek data consists of close to 45 reels of good data - more than for Sarsfeld.

IV. Performance Using Rogers Data

We have been working with the Rogers data base extracting features from subs and features for nonsubs. Much of the work involves finding peaks and flat places in the sonar return. Also, the target's travel is fitted with a polynomial to get an estimate of track aspect. Features extracted for subs are NP = number of peaks, NF = number of flat places, e = echo effective length, $ER^{3/2}$ = (echo energy) (Range)^{3/2}, and minimum distance between the largest peak and its nearest peak. A computer print out of these features for sub echoes⁺ and nonsub echoes⁺ are shown in Figures 3a and 3b. In Figure 3c, track aspect angles for the sub targets are shown. In figure 4a and Figure 4b is shown the actual computer output display of the first two sub echoes with peaks on the echo marked and with the above mentioned features displayed. In Figures 4c and 4d we see computer output displays for the first two nonsub echoes. Figure 4e shows the tracking ships track and the target track, while Figure 4f is a blow-up of the target track.

⁺ Sub echoes are denoted IOF and nonsub echoes ION in these figures.

V. Reverberation Correlation Calculations

A. Introduction

Given N sequential waveforms $\{v_{ij}(t)\}_{i=1}^N$ $_{j=1}^M$, from M corresponding band-pass stochastic processes $\{v_j\}_{j=1}^M$ obtained from M respective channels, it is desired to compute the M^2 possible[†] sample-ensemble-cross-covariance functions

$\{\Sigma_{mn}(t_1, t_2)\}_{n=1}^M$ $_{m=1}^M$ defined as follows:

$$\Sigma_{mn}(t_1, t_2) = \frac{1}{N} \sum_{s=1}^N [v_{sm}(t_1) - \bar{v}_m(t_1)][v_{sn}(t_2) - \bar{v}_n(t_2)] \quad (1)$$

where $\bar{v}_m(t_k)$ denotes the sample mean for m^{th} channel:

$$\bar{v}_m(t_k) = \frac{1}{N} \sum_{s=1}^N v_{sm}(t_k); \quad m = 1, 2, \dots, M \quad (2)$$

In a digital approach a discretized representation of the waveform $v_{ij}(t_k)$, $k = 1, 2, \dots, L$ will be available. If the stochastic sampling theorem is utilized, then the function $K_{mn}(t_1, t_2)$ is obtainable from signals $v_{ij}(t)$ sampled at a frequency N less than the Nyquist frequency, $f_s = 2(f_o + W/2)$; f_s is the sampling frequency, f_o is the bandpass center frequency, and W is the low-pass bandwidth of the stochastic processes $x^{(1)}$, $x^{(2)}$ (containing waveforms $x_{ij}^1(t)$ and $x_{ij}^2(t)$ respectively) in the Rice representation of v_j , i.e.,

$$v_{sj}(t) = x_{sj}^{(1)}(t) \cos \omega_o t - x_{sj}^{(2)}(t) \sin \omega_o t \quad (3)$$

$$v_{sj} \in v_j, \quad x_{sj}^{(1)} \in x_j^{(1)}, \quad x_{sj}^{(2)} \in x_j^{(2)}$$

If $f_o \gg W$, it may be practically impossible to sample at the resulting frequency f_s . Moreover, one is often interested in computing only the envelope of $\Sigma_{mn}(t_1, t_2)$ in which case sampling at f_s may be inefficient. An alternate method for computing this envelope denoted $\mathcal{E}(\Sigma_{mn}(t_1, t_2))$ or more briefly

$$\mathcal{E}_{mn}(t_1, t_2).$$

[†]There are $M(M+1)/2$ distinct cross-correlation functions.

is to quadrature sample the low pass functions $x_{ij}(t)$, $y_{ij}(t)$ at their Nyquist frequency of $W/2$ hz. One may then compute the $4M^2$ low-pass covariance functions $\sigma_{kl}^{mn}(t_i, t_j)$:

$$\sigma_{kl}^{mn}(t_i, t_j) = \frac{1}{N} \sum_{r=1}^N [x_{rm}^k(t_i) - \bar{x}_m^k(t_i)] [x_{rn}^l(t_j) - \bar{x}_n^l(t_j)]$$

$$k = 1, 2; \quad l = 1, 2; \quad n = 1, 2, \dots, M; \quad m = 1, 2, \dots, M \quad (4)$$

It is well-known that for jointly stationary stochastic processes y_m , that $\epsilon_{mn}(t_1, t_2)$ may be determined from the 4 low-pass functions $\sigma_{kl}^{mn}(t_1, t_2)$; $k = 1, 2$; $l = 1, 2$. Specifically:

$$\sigma_{kl}^{mn}(t_1, t_2) = \sigma_{kl}^{mn}(t_2 - t_1, 0) \quad l = 1, 2; \quad k = 1, 2$$

$$\sigma_{11}^{mn}(t_2 - t_1, 0) = \sigma_{22}^{mn}(t_2 - t_1, 0); \quad \sigma_{12}^{mn}(t_2 - t_1, 0) = -\sigma_{21}^{mn}(t_2 - t_1, 0)$$

$$\epsilon_{mn}(t_1, t_2) = \sqrt{[\sigma_{11}^{mn}(t_2 - t_1, 0)]^2 + [\sigma_{12}^{mn}(t_2 - t_1, 0)]^2} \quad (5)$$

Unfortunately, joint stationarity is a condition seldom met in many problems, e.g. Sonar.

B. Procedure

It is desired to sample a bandpass stochastic process at the lowest possible frequency which allows reconstruction, one such technique is Quadrature sampling. We may represent the sample bandpass function $x(t)$, bandwidth W as:

$$x(t) = x_1(t) \cos \omega_0 t - x_0(t) \sin \omega_0 t$$

where $x_1(t)$ and $x_0(t)$ are lowpass stochastic processes of which the highest frequency is $W/2$. Thus we may apply the stochastic sampling theorem to the lowpass processes and need sample $x_1(t)$ and $x_0(t)$ at W hz. each. The envelope of $x(t)$ is given by:

$$\varepsilon(x(t)) = \sqrt{x_1^2(t) + x_0^2(t)}$$

The phase is given by $\phi(x(t)) = \tan^{-1} \left[\frac{x_0(t)}{x_1(t)} \right]$. By choosing the sampling frequency f_s to be a submultiple of $\omega_0 \ni f_s \geq W$, we may obtain the samples of $x_1(t)$ by simply sampling $x(t)$ at frequency f_s . By taking another sample, exactly 90° after we take each sample of $x_1(t)$, we obtain the samples for $x_0(t)$. Thus we see that it is necessary to know ω_0 and to generate one set of samples at $f_s = \frac{\omega_0}{2\pi N}$ hz and another set delayed by $\frac{\omega_0}{4}$ radius. Given a synchronization signal $\cos \omega_0 t$, it is desired to generate a set of sampling pulses at a frequency $f_s = \frac{\omega_0}{2\pi N}$, N is an integer and another set delayed by $t_d = \frac{\omega_0}{4}$ radius. In the case of interest $\omega_0 = 18$ KHz, $N = 18$. Then $f_s = 1$ Hz and we may adequately sample a signal with a 1 KHz bandwidth. The delay between signals will be $t_d = \frac{1}{4} \times \frac{1}{18}$ msec. = $\frac{1}{72}$ msec.

In the original process, these samples were generated erroneously by sampling at 4 KHz and discarding the 3rd and 4th samples of every four thus obtained.

C. Description of Reverb Correlation Process

Four staves 1, 44, 47, 48 were quadrature sampled at 1 KHz, starting at 2 sec. after the zero time pulse to obtain 64 in phase and 64 quadrature samples for each staff. A total of 180 such sets of samples ($4 \times 180 = 720$ in phase vectors and 720 quadrature vectors) were obtained and stored on an IBM 1130 Magnetic Disk.

The correlation coefficient functions were computed for four different subsets of the 180 vectors (# 1-60, # 60-121, #121-180, and # 1-180) in order to examine the nonstationarity of the process. For each such ensemble, the 66 possible distinct correlation coefficients were computed as follows. For each pair of the four staves, there are two in phase and two quadrature vectors. For each of these four vectors, the means were computed and then subtracted out. The four 64×64 covariance matrices were then computed. These were then combined using the relation derived earlier to obtain the sampled envelope of the cross covariance function for that pair of staves $\underline{\Sigma}^{(m)(n)}$. The correlation coefficient matrix p^{mn} was then computed using the relation:

$$p_{ij}^{mn} = \frac{\sigma_{ij}^{mn}}{\sqrt{\sigma_{ij}^{mn} \sigma_{jj}^{mn}}}$$

D. Experimental Staff Correlations

We were asked by Naval Ships System Command to investigate correlations among multistave data. The procedure for numbering staves is shown in Figure 5.

Echos or pings were from 3 different modes. The ping numbers and corresponding modes are shown below:

Ping #	Pulse Width (at $7\frac{1}{2}$ ips)
1 - 48	60 m. sec. c.w.
49-100	Chatterbox (~ pulses, each ~ 10 m. sec.)
101-180	Mixed c.w. (4 short followed by two 60 m.sec.)

Signals for the various staves were recorded on 14 channel tape as illustrated in Figure 5. A general block diagram of the procedure is shown in Figure 7. A sequence of pictures shown in Figure 8 show the reverberation correlations across staves for several configuration. A sequence of such pictures are in the procession of Navel Ships System Command.

Part II

FORWARD (Next 90 Days)

We are processing more of the Rogers data so as to report more performance results. We will derive features for the nonsubmarine target such as sea weed where there are multiple echoes in either range, bearing, or both range and bearing. We are inserting a priori knowledge concerning existence of two major peaks for subs and peak signal power/average noise. Sometime soon we must begin to give attention to "false targets" and video scan data to achieve a more accurate estimate of target bearing. This estimate of target bearing is important when estimating target spaced and target length.

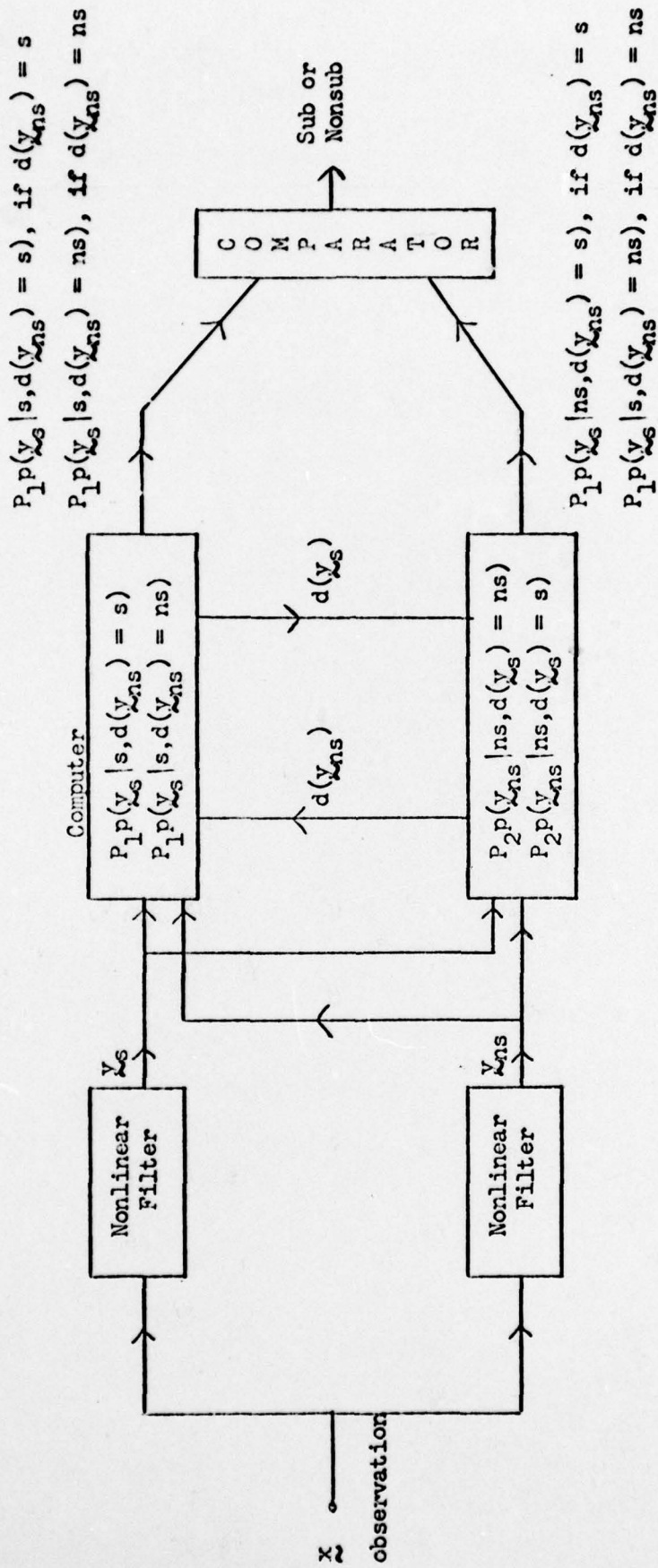


Figure 1: Nonlinear Filters for Automatic Detection

Figure 2: ROGERS DATA Austin 6/21/70

Run #	PME Reel #	PME Start	Footage Stop	Purdue Reel #	Rotation Start	Ctr Stop	Spd	Cls	Aspect	# of Pings	Comments
1	9	1570	1692	ROG-1	0041	0111	15	S	Bow 015-320	50	Rng. & Bng to Lag. edge
2	11	370	485	ROG-1	0129	0201	13.5	S	Beam	40	No Good
3	13	0	165	ROG-1	0204	0324	15	S	Beam twd. Bow		Retake
4	13	0	165	ROG-1	0330	0454	15	S	Beam twd. Bow	28	No Good
5	15	2320	2500	ROG-1	0458	0485	13	S	Quarter & Beam	30	Retake
6	15	2320	2500	ROG-1	0488	0628	13	S	Quarter & Beam	30	No Good
7	18	1452	1566	ROG-1	0631	0709	16	S	Stern Quarter	25	Retake
8	18	1452	1566	ROG-1	0712	0899	16	S	Stern Quarter	25	No Good
9	21	1557	1665	ROG-1	0903	1031	16	S	Port Bow & Stbd Bow	30	Retake
10	23	1170	1262	ROG-1	1036	1132	15	S	Direct Bow	16	
11	23	1375	1470	ROG-1	1136	1248	15	S	Brd. Bow-Beam	37	Last Two may be FM
12	23	2076	2180	ROG-1	1255	1470	15	S	Beam-Bow	70	
13	25	0958	1088	ROG-1	1473	1612	15	S	* Brd Bow-Dir. Bow	35	
14	28	0858	1187	ROG-1	1617	1957	10	S	Stern Bow	91	
15	48	1325	1461	ROG-1	1959	2127	15	S	240-210	35	
16	16	2328	2512	ROG-1	2135	2363	15.5	S	Stern-Stbd Beam	30	Very weak
17	22	0710	0819	ROG-1	2311	2530	17	S		30	Weak
18	41	1782	1904	ROG-1	2537	2743	18	S	Bow-Brd. Bow	40	Intermittent at max rng.
19	6	1645	1720	ROG-2	0010	0072	14	N	?	20	Good S/N
20	51	2356	2446	ROG-2	0077	0145	15	N	?	33	"
21	63	1546	1706	ROG-2	0149	0262	6	N	?	30	"
22	64	1576	1667	ROG-2	0266	0336	7	N	?	30	Very sublike
23	64	1965	2054	ROG-2	0340	0413	13.7	N	?	30	Very sublike
24	65	1578	1668	ROG-2	0418	0492	13.5	N	?	30	Good S/N

*

Figure 2 continued

Run #	PME Reel	PME Start	Footage Stope	Purdue Reel #	Rotation Start	Ctr Stop	Spd	Cl.	Aspect	# of Pings	Comments
25	67	1822	1910	ROC-2	0497	0569	13.5	N	?	30	Good S/N
26	67	2224	2314	ROC-2	0574	0644	13.5	N	?	30	"
27	26	0331	0538	ROC-2	0648	0785	13.5	N	?	50	med-weak inconsistent
28	26	0228	0315	ROC-2	0788	1043	13.5	N	?	20	weak to very weak

Figure 3a
Subs

Class	Ping	$\hat{\lambda}_e$	NP	NF	Δ	$\frac{3}{2}$ ER	
IOF	1	222	9	6	13	0.43953418E	10
IOF	2	183	8	3	16	0.17846935E	10
IOF	3	185	10	2	14	0.24297031E	10
IOF	4	189	12	0	14	0.23733504E	10
IOF	5	177	8	2	13	0.37908367E	10
IOF	6	161	7	2	15	0.16971312E	10
IOF	7	163	5	4	17	0.21764265E	10
IOF	8	224	10	6	17	0.33720611E	10
IOF	9	209	13	2	13	0.24744596E	10
IOF	10	153	5	6	16	0.16144578E	10
IOF	11	176	7	5	18	0.15854041E	10
IOF	12	189	8	1	11	0.39064043E	10
IOF	13	221	14	5	15	0.36873088E	10
IOF	14	164	4	7	16	0.15878937E	10
IOF	15	144	7	5	12	0.21061847E	10
IOF	16	166	9	0	14	0.20330437E	10
IOF	17	103	5	1	21	0.20492848E	10
IOF	18	156	7	1	16	0.28137395E	10
IOF	19	142	5	2	14	0.19227906E	10
IOF	20	213	10	4	12	0.64481341E	10
IOF	21	203	11	6	13	0.51928535E	10
IOF	22	169	8	4	16	0.30139898E	10
IOF	23	268	13	1	14	0.65371965E	10
IOF	24	217	12	0	14	0.50553641E	10
IOF	25	218	10	2	10	0.43095306E	10
IOF	26	152	7	3	10	0.23599979E	10
IOF	27	143	7	2	13	0.20427865E	10
IOF	28	189	7	5	15	0.25379491E	10
IOF	29	208	11	2	15	0.29854699E	10
IOF	30	177	6	6	22	0.26129017E	10
IOF	31	199	9	5	14	0.23576181E	10
IOF	32	201	12	0	13	0.43703255E	10
IOF	33	174	9	3	15	0.24018805E	10
IOF	34	213	9	6	14	0.46613770E	10
IOF	35	199	8	2	18	0.16345891E	10
IOF	36	192	7	5	16	0.26328268E	10
IOF	37	193	10	5	12	0.34851179E	10

Figure 3b
Subs

10F	38	326	11	17	13	0.44666491E	10
10N	1	450	25	10	8	0.19924640E	09
10N	2	263	4	16	28	0.93187635E	09
10N	3	146	4	4	16	0.90724403E	09
10N	4	182	4	10	14	0.94710118E	09
10N	5	351	8	25	14	0.95191552E	09
10N	6	341	8	20	15	0.87393958E	09
10N	7	230	8	12	12	0.91324620E	09
10N	8	197	7	7	13	0.88783616E	09
10N	9	243	8	11	16	0.99487104E	09
10N	10	213	8	5	17	0.10935014E	10
10N	11	283	10	9	15	0.10429190E	10
10N	12	253	11	2	12	0.11193592E	10
10N	13	348	11	16	23	0.91403609E	09
10N	14	435	16	14	12	0.99097190E	09

Ping Number	Aspect Angle (Track)
1	115
2	114
3	113
4	112
5	112
6	110
7	110
8	110
9	109
10	109
11	110
12	110
13	106
14	106
15	106
16	106
17	105
18	104
19	103
20	102
21	102
22	102
23	100
24	100
25	100
26	98
27	98
28	98
29	97
30	96
31	96
32	93
33	94
34	94
35	94
36	92
37	91
38	90

Figure 3c: Track Aspect for Subs

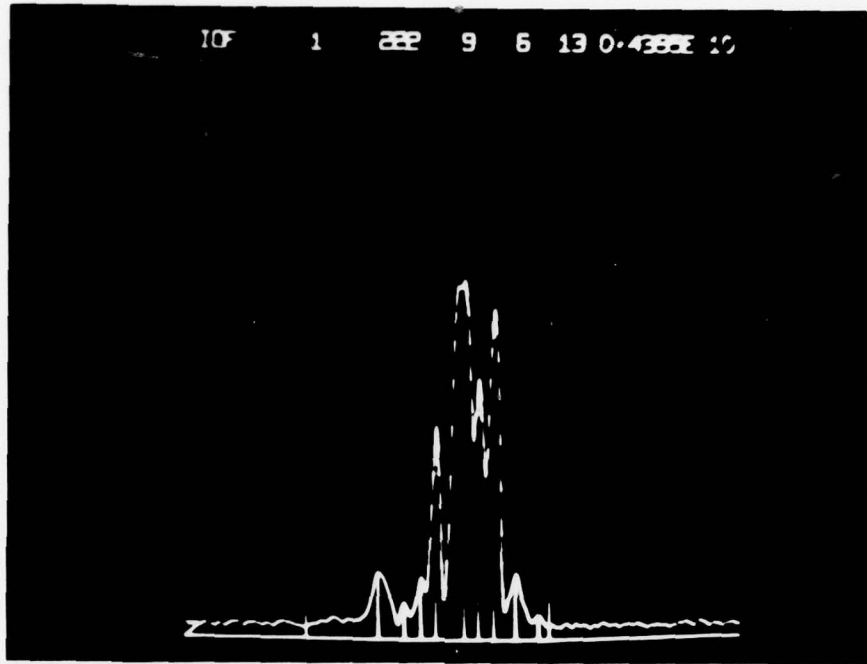


Figure 4a: Sub Echo, Features, and Marked Peaks

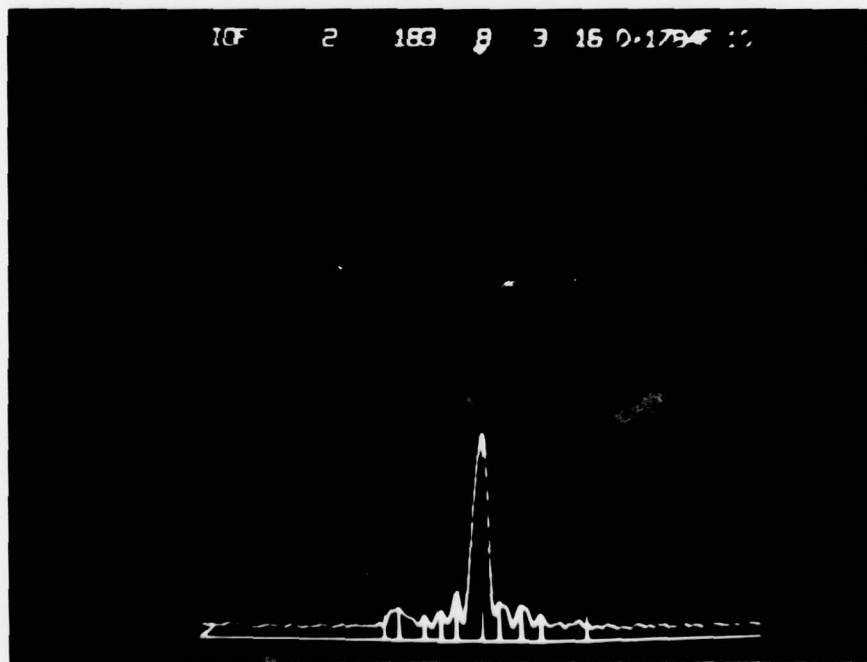


Figure 4b: Sub Echo

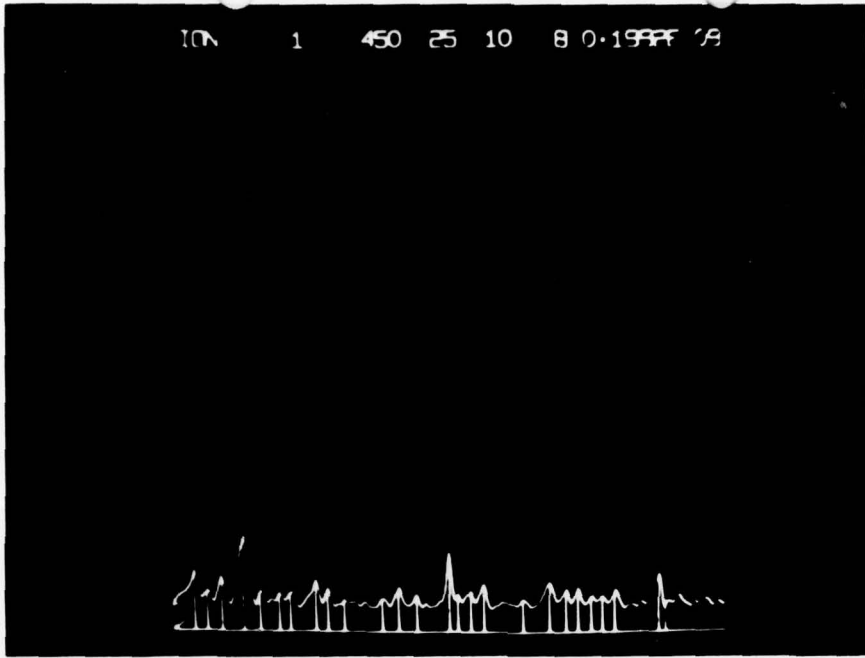


Figure 4c: Nonsub Echo

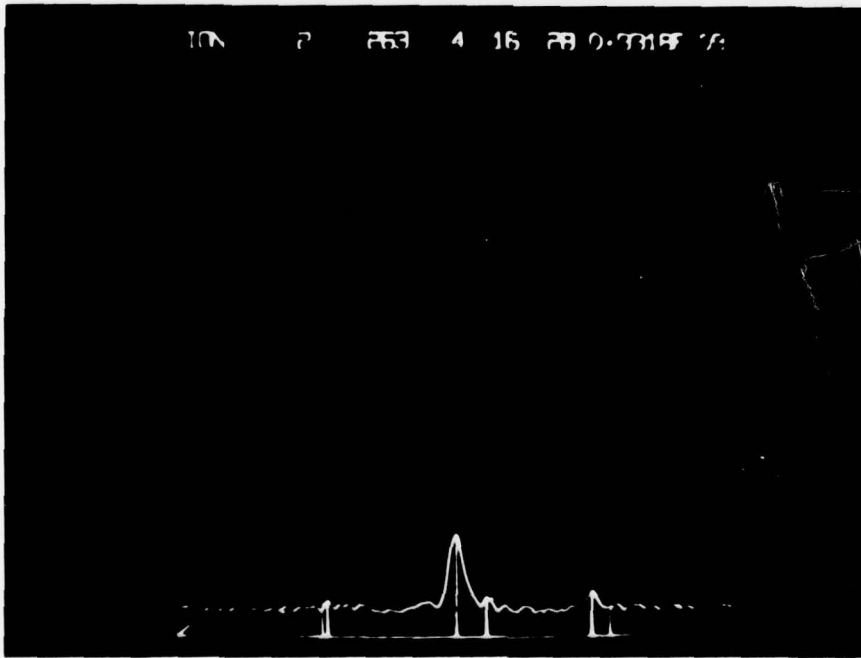


Figure 4d: Nonsub Echo

$$\epsilon_{mn}(t_1, t_2).$$

⁺ There are $M(m+1)/2$ distinct cross-correlation functions.

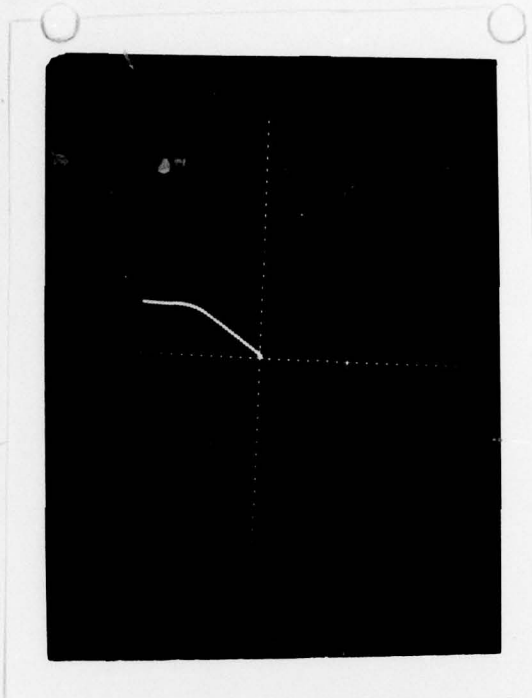


Figure 4e: Top shows Tracking Ship Track While Bottom Shows Target Track



Figure 4f: Enlarged View of Target Track Shown in Figure 4e.

RELATIVE STAVE LOCATIONS

SHIP'S HEADING



STAVE NUMBERS

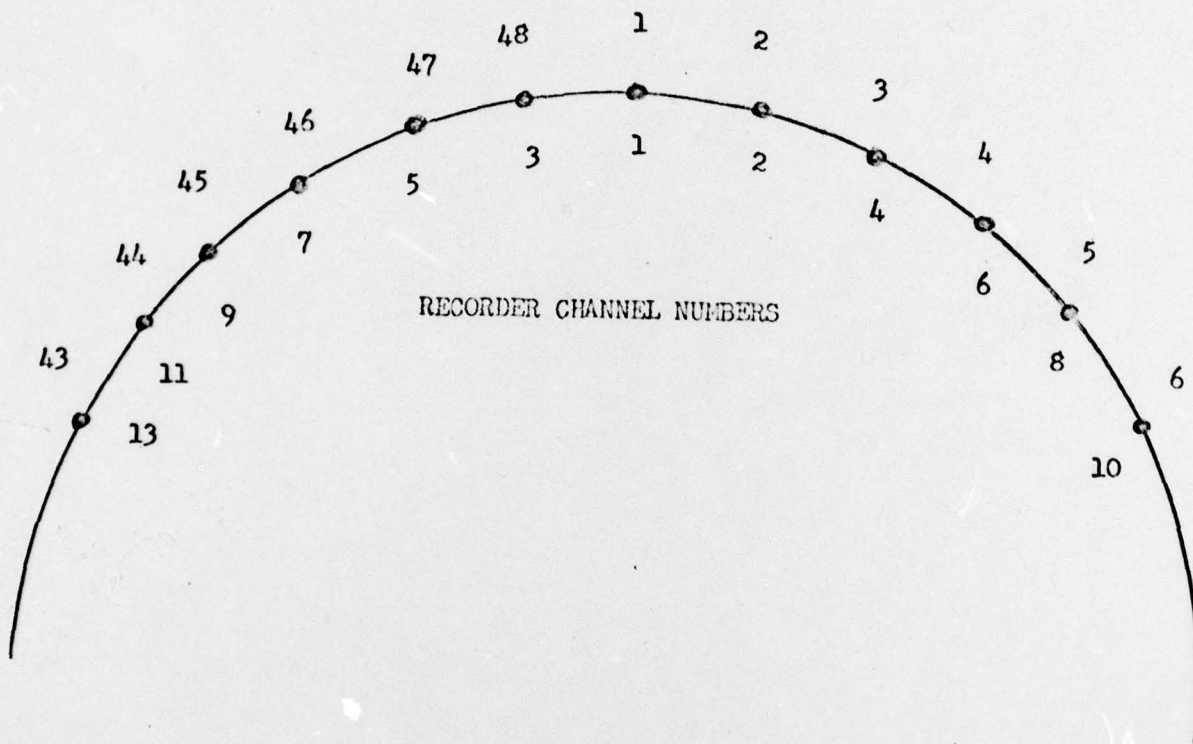


Figure 5: STAVE LAYOUT FOR TAPE # RVB-1

$f_0 = 17.95 \text{ KHZ}$

Bandwidth = 500 HZ

does not agree with 17.95 earlier

<u>Channel</u>	<u>Method</u>	<u>Signal</u>
1	Direct	Stave #1
2	Direct	Stave #2
3	Direct	Stave #4?
4	Direct	Stave #3
5	Direct	Stave #47
6	Direct	Stave #4
7	Direct	Stave #46
8	Direct	Stave #5
9	Direct	Stave #45
10	Direct	Stave #6
11	Direct	Stave #14
12	FM	12.95 KHZ reference
13	Direct	Stave #13
14	FM	1 sec pulse; starts when beam is dead ahead

Recorded @ $7\frac{1}{2}$ ips.

Set footage counter to zero @ first trace of audio on stave channels;
then

<u>ft.</u>	<u>Pings</u>
0-438	1-48 Single ping CW, Long pulse (60 m.sec)
456-938	49-100 Chatterbox (10 closely spaced pings)
953-1505	101-178 13 burst of 4 long, two short CW

Figure 6: MULTI-STAVE REVERBERATION DATA

Figure 7: REVERB CORRELATOR

